Supplementary Material (ESI) for New Journal of Chemistry

Electronic Supplementary Information

(ESI)

Electrochemical Modification of Chromium Surfaces using 4-Nitro- and 4-Fluorobenzenediazonium Salts

Mogens Hinge,[a] Marcel Ceccato,[a] Peter Kingshott,[b] Flemming Besenbacher,[b] Steen Uttrup Pedersen,*[,a,b] and Kim Daasbjerg*[,a,b]

[a] *Department of Chemistry, Aarhus University, Langelandsgade 140, DK-8000 Aarhus C, Denmark*

[b] *Nanoscience Center (iNANO), Institute of Physics and Astronomy, Ny Munkegade, DK-8000 Aarhus C, Denmark*

Experimental

Chemicals. Synthesis of 4-nitrobenzene and 4-fluorobenzenediazonium tetrafluoroborates followed the general procedure outlined elsewhere.[1S] Further purification consisted of dissolving it in acetonitrile, precipitation by addition of diethyl ether and after filtration and vacuum drying, storing it at –18 °C. 2,4,6-Triphenylthiopyrylium tetrafluoroborate was prepared according to the method outlined in literature.[2S] Acetonitrile (anhydrous, 99.9%) was purchased from Lab-Scan. Tetrabutylammonium tetrafluoroborate (Bu_4NBF_4) was prepared using standard procedures. All other compounds were commercial and used in the highest grade available. Prior to use the electrolyte solution, 0.1 M Bu_4NBF_4/CH_3CN, was dried by letting it run through a column containing Al_2O_3 (Sigma Aldrich, 99.99%). Al_2O_3 had further been activated by heating in a vacuum oven at 450 °C.

Electrodes and Instrumentation. A standard 3-electrode electrochemical setup was employed. Two different chromium substrates were used according to the specific purpose of the measurements. For cyclic voltammetric measurements the working electrode (~2 mm × ~3.5 mm) was made from chromium nuggets and polished with diamond suspensions (Struers, grain size: 9, 3, 1, and 0.25 μm) followed by rinsing with water and ethanol and finally 10 min ultrasonic cleansing in acetone. A picture of the electrode tip and a scanning electron microscopy (SEM) image of the polished surface is shown in Figure S1.

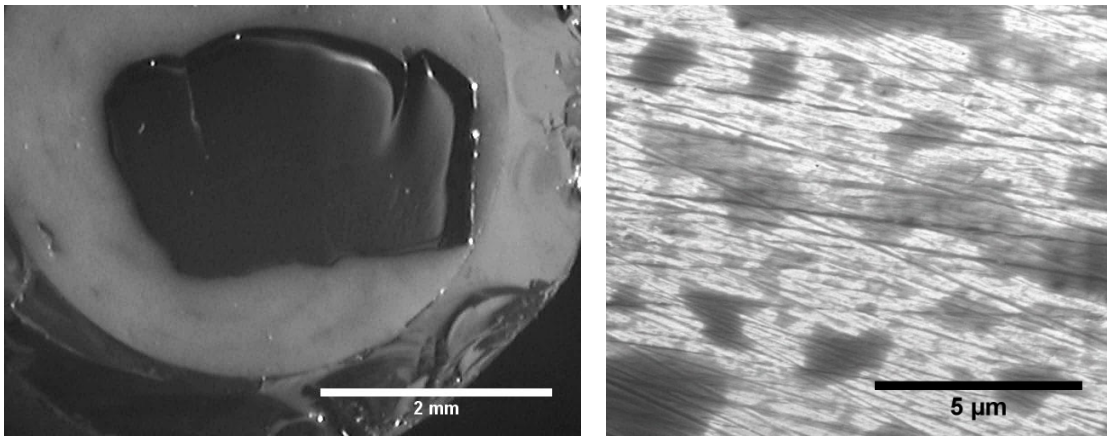

Figure S1. Picture of electrode tip (left), where the black part in the centre is the polished chrominum nugget inbedded in white epoxy within a glass tube and an SEM image of the surface (right).

It can be seen from the SEM image in Figure S1 (right) that the surface, although looking smooth on visual inspection (left), still have a microscopic surface roughness after polishing. Thus, the actual surface area is significantly larger than the geometrical area.

For preparation of samples used for spectroscopical analysis the working electrode consisted of chromium deposited on microscope glass slides (1.1 cm × 6 cm) by physical vapour deposition. For both kinds of electrodes a Ag/AgI electrode (silver wire immersed in a Pyrex tube containing 0.1 M Bu_4NBF_4 + 0.01 M Bu_4NI in acetonitrile) separated from the main solution by a ceramic frit served as reference electrode. At the end of each experiment the standard potential of the ferrocenium/ferrocene couple, $E^0_{Fc^+}$, was measured and all potentials were referenced against SCE using a previous determination of $E^0_{Fc^+}$ = 0.41 V vs. SCE in acetonitrile.[3S] The auxiliary electrode consisted of a platinium wire. Electrochemical data were recorded on a CH Instruments 601C electrochemical workstation.

Electrografting. Grafting was carried out by means of 3 successive voltammetric cycles from 0.15 to –0.85 V vs. SCE on a 2 mM 4-nitrobenzenediazonium tetraflouroborate solution in 0.1 M Bu_4NBF_4/CH_3CN. The grafted surface was thoroughly rinsed and ultrasonicated for 10 min in acetone before further analysis. It was noted that a potentiostatic electrolysis performed at a potential of –0.5 V vs. SCE for 300 s rather than 3 successive cyclic voltammetric cycles produces a relatively thicker film. A similar procedure was employed in the grafting of 4-fluorobenzenediazonium tetrafluoroborate.

Polarization Modulation Infrared Reflection Absorption Spectroscopy (PMIRRAS). PMIRRAS spectra were recorded on a Bio-Rad FTS 65A (Randolph, MA) FTIR-spectrometer equipped with an External Experiment Module with a narrow band mercury-cadmium-telluride (MCT) detector cooled in liquid nitrogen. The infrared beam was modulated at 37 kHz between *s* or *p* polarization by combining a gold wire polarizer with Hinds zinc-selenide photoelastic modulator (PEM-90/II/ZS37). The PEM was adjusted so the *s* polarization was linear for wavenumbers around 1500 cm^{-1}. The chromium substrates were irradiated with an incident grazing angle of 80°. The two signals, $R_p - R_s$, and, $R_p + R_s$, were extracted with a high-pass filter (EG&G model 189) and a lock-in amplifier (SR 810 DSP) and digitized sequentially as 20 spectra of each signal in 20 cycles (in total 800 spectra). The differential surface reflectivity [$\Delta R/R = (R_p - R_s)/(R_p + R_s)$] spectra were obtained with 4 cm^{-1} resolution. The experimental PMIRRAS spectra were normalied with respect to that of a bare substrate and finally baseline-corrected

using the facilities of the Digilab Resolution Pro 4.0 program. All spectra were recorded at room temperature in dry atmosphere.

X-ray Photoelectron Spectroscopy (XPS). A Kratos Axis Ultra-DLD instrument operated with a monochromatic Al K(alfa) X-ray source at a power of 75 W was employed for the XPS analysis. Survey scans were acquired by accumulating two sweeps in the 0–1400 eV range at a pass energy of 160 eV. High-resolution scans were acquired at a pass energy of 20 eV. The pressure in the main chamber during the analysis was in the range of 10^{-8} mbar. The generated data were processed using the CasaXPS software. Atomic surface concentrations were determined by fitting the core spectra using Gaussian line shapes and a linear background and binding energies of the components in the spectra were determined by calibrating against the C-H/C-C peak in the C1s spectra at 285.0 eV. The systematic error is estimated to be of the order of 5–10%.

Scanning Electron Microscopy (SEM). All SEM images were made on a FEI NOVA nanoSEM 600 in high vacuum mode (0.96 mPa) with an acceleration voltage of 5 kV, spot size 3, and 108 μA at a working distance of ~3 mm. SEM images was made in field immersion mode with a through lens detector (TLD) on samples grounded with colloidal carbon paste. The SEM is controlled by the software program xT Microscope Control.

Results and Discussion

Blocking experiments. Blocking properties of a 4-nitrophenyl-modified chromium electrode, Cr-NB (obtained by means of 3 successive voltammetric cycles from 0.15 to –0.85 V vs SCE on a 2 mM 4-nitrobenzenediazonium tetraflouroborate solution in 0.1 M Bu_4NBF_4/CH_3CN), are deduced from the recording of cyclic voltammograms of the redox probe 2,4,6-triphenylthiopyrylium tetrafluoroborate in 0.1 M Bu_4NBF_4/CH_3CN (Figure S2). A cyclic voltammogram of Cr-NB recorded in a pure electrolyte solution is included in Figure S2.

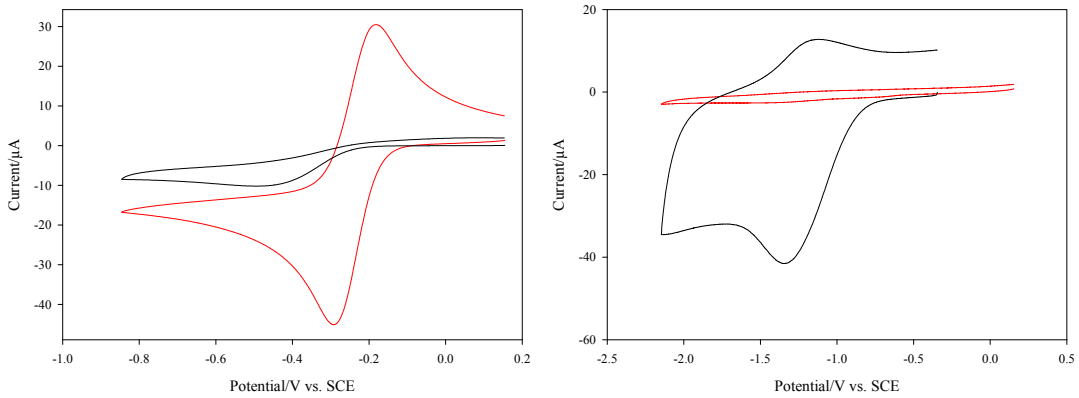

Figure S2. Cyclic voltammograms recorded in 0.1 M Bu_4NBF_4/CH_3CN containing 2 mM 2,4,6-triphenylthiopyrylium tetrafluoroborate (left) and no redox probe (right) at a sweep rate of 0.1 V s^{-1}; freshly polished chromium electrode (——) and an electrode modified with 4-nitrobenzenediazonium tetrafluoroborate (——).

Evidently, the charge transfer between Cr-NB and 2,4,6-triphenylthiopyrylium tetrafluoroborate becomes severely hindered, if electrografting using cyclic voltammetric reduction of 4-nitrobenzenediazonium salt is employed. Using electrolysis for an extended period rather than cyclic voltammetry as the electrografting procedure, the modified layer becomes thicker and even more blocking, resulting in a complete lack of electrochemical signal from the redox probe (data not shown). Noteworthy, even for a freshly polished chromium electrode the electrochemical response is quasi-reversible (peak separtion = 110 mV) which we attribute to the presence of a thin and somewhat electrical insulating outer layer of chromium oxide. Furthermore, it can be seen from the voltammograms recorded at an ungrafted electrode in a pure electrolyte solution without redox probe that no reduction of the chromium surface takes place in the entire potential range. In contrast, for the grafted electrodes signals from the surface-attached redox couple $-C_6H_4NO_2/-C_6H_4NO_2^{\bullet-}$ are evident.

PMIRRAS. Samples for these measurements were prepared from microscope glass slides upon which an oriented chromium coating was deposited by physical vapour deposition. This has the consequences that absorption bands will point downwards and not upwards as usual and the intensity of the bands be dependent on the sample orientation. In Figure S3 spectra have been recorded at various angles of the grafted chromium substrate Cr-NB.

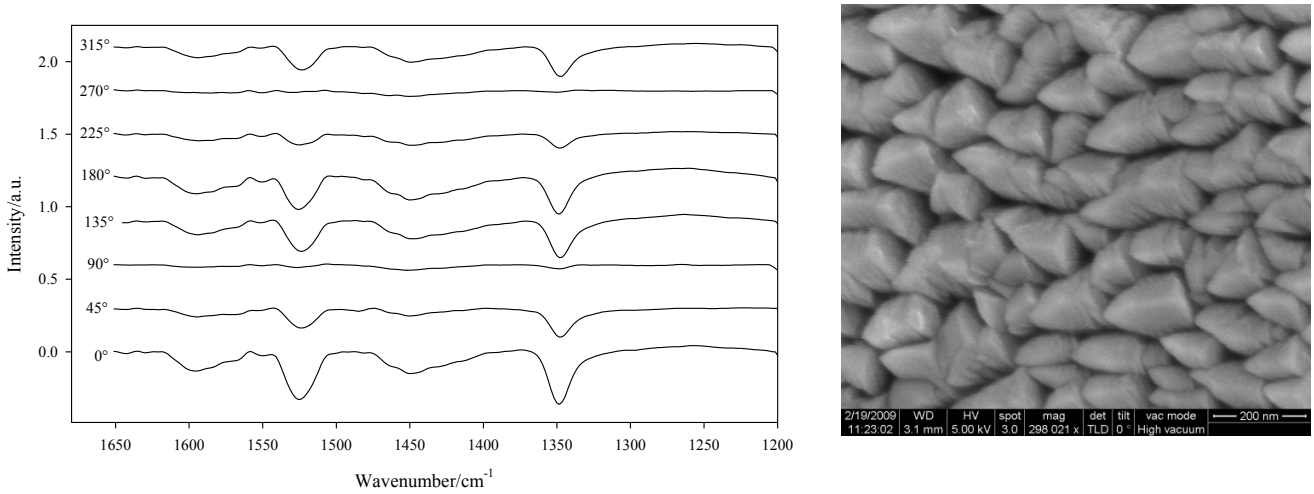

Figure S3. PMIRRAS spectra recorded on a chromium-coated microscopic glass slide grafted with 4-nitrobenzenediazonium tetrafluoroborate, Cr-NB (left). The zero angle corresponds to the situation, where the glass slide is placed horizontal in the sample holder as illustrated in the SEM image (right).

As seen from Figure S3 (right) the surface of the deposited chromium substrate has a predominant orientation. This orientation changes the polarization of the incedent light giving arise to a change in the *p* polarization. The consequences of this are that absorption bands will point downwards and the intensity of the bands will be dependent on the sample orientation (Figure S3; left). Notably, the signal is almost completely vanished for orientations of 90° and 270°, at which the individual signals from the *p* and *s* polarizations become equal. Based on these observations we choose to carry out all PMIRRAS measurments at angles of either 0° or 180.

XPS. In Figure S4 survey scans for the ungrafted, Cr-NB, and Cr-FB electrodes are collected.

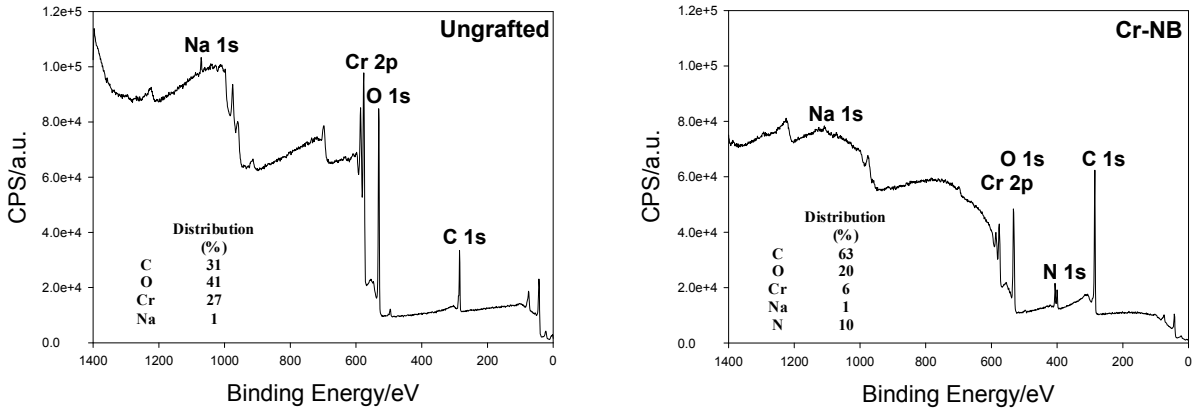

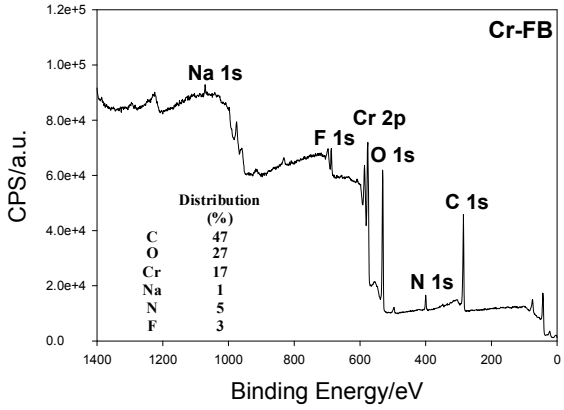

Figure S4. XPS survey scans for the ungrafted (i.e., a chromium-covered microscopic glass slide; top left), Cr-NB (top right), and Cr-FB (bottum) electrodes.

Signals from the elements carbon, chromium, and oxygen are found for all three types of electrodes, including the ungrafted one. This is due to the fact that adsorption of organic molecules from air inevitably will occur on the samples, unless highly specialied precautions are made. Importantly, large amounts of N and F are found only in the survey scans for Cr-NB and Cr-FB with their nitrophenyl and fluorophenyl groups, respectively.

High resolution spectra of chromium and nitrogen for the ungrafted, Cr-NB, and Cr-FB electrodes are collected in Figure S5.

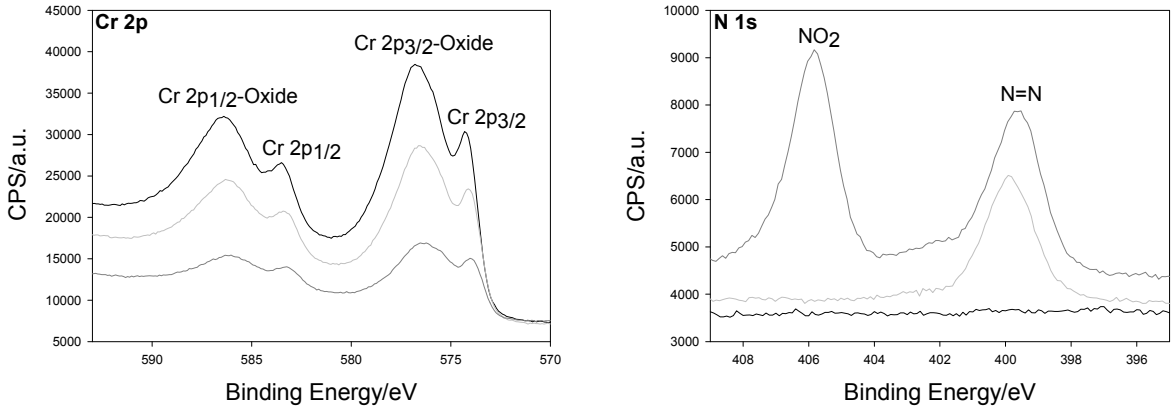

Figure S5. High resolution carbon XPS spectra of chromium (left) and nitrogen (right) for the ungrafted (i.e. a chromium-covered microscopic glass slide; black line), GC-BF (light gray line), and GC-NB (gray line) electrodes.

For the ungrafted sample Cr 2p signals originating from the chromium metal and, in particular, chromium oxides are observed. This is in accordance with expectation in that chromium in the presence of (atmospheric) oxygen immediately will be covered with a thin oxide layer. The grafted surfaces show the same signals, although the intensity is lower because of the presence of an upper organic layer.

The high resolution XPS spectrum for N 1s reveals the presence of two types of nitrogen. Undoubtedly, the N 1s peak at 406 eV for Cr-NB corresponds to that of nitrogen in a nitro group,[4S,5S] while a minor N 1s peak around 400 eV could originate from partially reduced nitro groups (i.e. hydroxylamino or amino groups)[4S,5S] or azo groups.[6S-8S] The resolution of the XPS spectra is too low to differentiate between these types of nitrogen.

Finally, in Figure S6 the fitting of the high resolution XPS spectrum of Cr-NB is shown along with a tabulation of the various contributions.

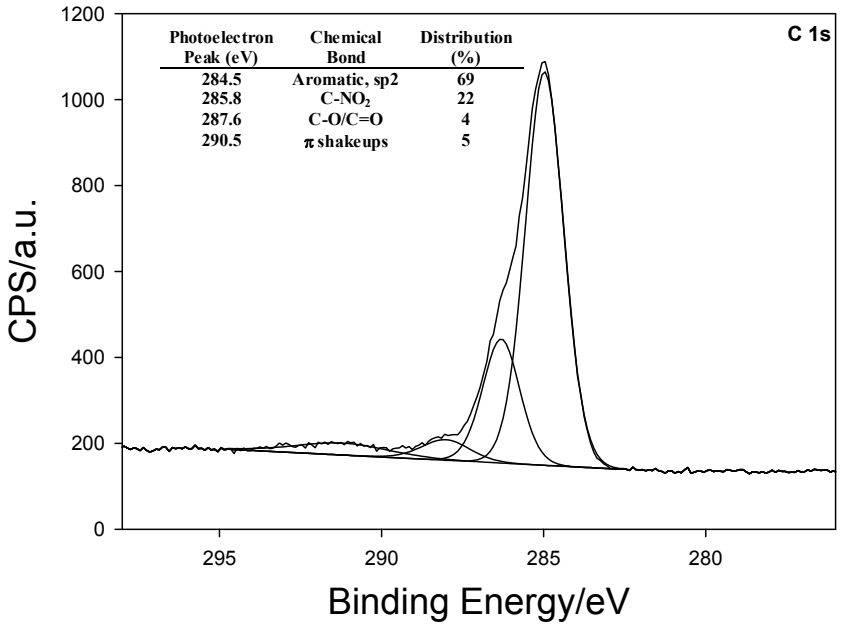

Figure S6. Elaboration of the high resolution carbon XPS spectra for GC-NB.

References

(1S) Klamann, D. *Metoden der Organischen Chemie*, 4th ed.; Padeken, H.-G., Ed.; Georg Thieme Verlag: Stuttgard, Germany, 1990; Vol. 2, Chapter 5, 1060.

(2S) Wizinger, R. Ulrich, P. *Helv. Chem. Acta* **1956**, *39*, 207.

(3S) Daasbjerg, K.; Pedersen, S. U.; Lund, H. In *General Aspects of the Chemistry of Radicals*; Alfassi, Z. B., Ed.; Wiley: Chichester, U.K., 1999; 385.

(4S) Adenier, A.; Cabet-Deliry, E. Chauss, A.; Griveau, S.; Mercier, F. ; Pinson, J. ; Vautrin-Ul, C. *Chem. Mater.* **2005**, *17*, 491.

(5S) Mendes, P.; Belloni, M.; Ashworth, M.; Hardy, C.; Nikitin, K.; Fitzmaurice, D.; Critchley, K.; Evans, S.; Preece, J. *ChemPhysChem* **2003**, *4*, 884.

(6S) Saby, C.; Ortiz, B.; Champagne, G. Y.; Bélanger, D. *Langmuir* **1997**, *13*, 6805.

(7S) Doppelt, P.; Hallais, G.; Pinson, J.; Podvorica, F.; Verneyre, S. *Chem. Mater.* **2007**, *19*, 4570.

(8S) Shewchuk, D.M.; McDermott, M.T. *Langmuir* **2009**, 25, 4556.